

SECOND-ORDER DISPERSION MEASUREMENT IN LHC

J. Keintzel*¹, J. Coello de Portugal-Martinez, J. Dilly, E. Fol, A. Garcia-Tabares, M. Hofer¹,
E. Maclean, L. Malina, T. Persson, R. Tomás, A. Wegscheider
1211 CERN, Geneva 23, Switzerland

¹also at Vienna University of Technology, 1040 Vienna, Austria

Abstract

The quadratic dependence of the orbit on the relative momentum offset, also known as second-order dispersion, is analysed for the first time for the LHC. In this paper, the measurement and analysis procedure are described. Results and implications on future optics are discussed.

INTRODUCTION

The dependence of the orbit change Δz

$$\Delta z = \eta_{z,1} \delta_p + \eta_{z,2} \delta_p^2, \quad (1)$$

on the relative momentum offset $\delta_p = \frac{\Delta p}{p}$ is known as the dispersion function, where $\eta_{z,1}$ and $\eta_{z,2}$ refer to the linear and second-order dispersion, respectively, and z is one of the transverse coordinates x or y . $\eta_{z,1}$ is generated by dipoles and quadrupoles, and in an ideal flat machine where dipoles bend only horizontally, the vertical dispersion is zero. In a machine like the LHC, however, vertical dispersion is generated through crossing angle bumps close to the Interaction Point (IP) and therefore vertical bending [1], as well as through betatron coupling or misalignments of quadrupoles. A general equation of motion of z including elements up to third order can be found in [2]. With the approximation given in Eq. (1), it is possible to derive simplified differential equations of motion. An approach for a general solution for higher-order dispersion is given in [3]. By neglecting coupling and vertical bending it reads

$$\eta_{x,1}(j) = \frac{\sqrt{\beta_x(j)}}{2 \sin(\pi Q_x)} \sum_i \kappa \sqrt{\beta_x(i)} \cos(\phi_{x,ij} - \pi Q_x), \quad (2)$$

$$\eta_{x,2}(j) = \frac{\sqrt{\beta_x(j)}}{2 \sin(\pi Q_x)} \sum_i \left(-\kappa - \frac{1}{2} m \eta_{x,1}^2(i) + k \eta_{x,1}(i) \right) \sqrt{\beta_x(i)} \cos(\phi_{x,ij} - \pi Q_x), \quad (3)$$

$$\eta_{y,1} = \eta_{y,2} = 0, \quad (4)$$

where $\kappa = 1/\rho$ with the dipole bending radius ρ , k and m are the normalised quadrupole and sextupole strengths, respectively, β refers to the β -function, Q_x to the horizontal tune and $\phi_{x,ij} = \phi_{x,j} - \phi_{x,i}$ when $j > i$ or $\phi_{x,ij} = \phi_{x,j} - \phi_{x,i} + 2\pi Q_x$ when $j < i$ to the phase advance between the longitudinal positions i and j . The sum extends over all dipoles, quadrupoles and sextupoles, where for large machines like the LHC, higher-order terms in κ and terms

* jacqueline.keintzel@cern.ch

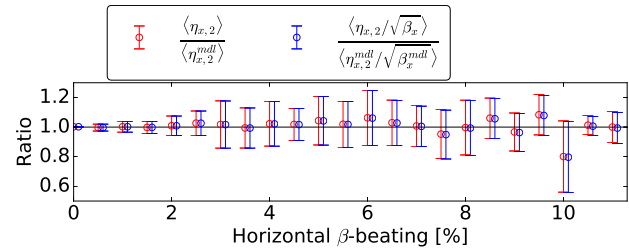


Figure 1: Average of optics functions ratios over β -beating.

including the dispersion deviation with respect to the longitudinal position, $\eta'_{x,1}$, have been neglected [3]. The derived Eqs. (2)-(4) agree with [4], divided by a factor 2. It has to be noticed that Eqs. (2)-(4) need to be adapted in the presence of linear coupling. As expected, $\eta_{x,1}$ is generated by linear field terms, whereas higher-order fields generate $\eta_{x,2}$. In addition, field errors, present in magnetic elements, coupling, as well as feed-down through misaligned elements, impact the orbit and therefore the second-order dispersion [2, 5].

Normalised dispersion $\omega_{z,n}$ can be measured independently of Beam Position Monitor (BPM) calibration errors [6]. The averages of $\eta_{x,2}$ and $\omega_{x,2}$ are constant over a large range of β -beating, generated by applying increasing field errors to model simulations, as seen in Fig. 1, where the superscript *mdl* refers to an error-free model. Regarding the measurements, $\eta_{z,n}$ is obtained by a fit of the closed orbit (CO) over δ_p , and scaled as

$$\omega_{z,n} = \frac{\eta_{z,n} \langle \omega_{z,1}^{mdl} \rangle}{A_z \langle \frac{\eta_{z,n}}{A_z} \rangle}, \quad (5)$$

where A_z is the measured mean amplitude of the betatron oscillation, n the order of the dispersion and the linear model normalised dispersion $\omega_{z,1}^{mdl} = \eta_{z,1}^{mdl} / (\beta_z^{mdl})^{1/2}$. In an ideal flat machine, $\langle \eta_{y,1}^{mdl} \rangle$ is zero, thus leading to vanishing $\omega_{y,n}$, which is therefore not discussed. Nevertheless, future optics measurements of ballistic optics [7] with non-zero $\langle \eta_{y,1} \rangle$ can be performed to analyse $\omega_{y,n}$.

In the presence of dispersion, the transverse position of a particle reads [5]

$$z = \sqrt{2\beta_z J_z} \cos \varphi_z + \Delta z, \quad (6)$$

with the action J_z and the angle variable φ_z . In Gaussian beam distributions $\langle z^2 \rangle = \sigma_z^2$, with the transverse beam size σ_z . Assuming δ_p follows a Gaussian distribution with the maximum at $\delta_p = 0$, it follows that $\langle \delta_p^n \rangle = 0$ for odd n and $\langle \delta_p^2 \rangle = \sigma_p^2$. If δ_p is uncorrelated to $2\langle J_z \rangle = \epsilon_z$ and φ_z it

Table 1: Analysed measurements and their parameters, for both beams, where n and d indicate the natural and driven tune, respectively, where only the fractional part is given. Xing: Half crossing angle. IP: Interaction Point. E: Centre-of-mass energy. ATS: Achromatic Telescopic Squeezing optics [8]. VdM: Van der Meer optics. In IP1 and IP2 the beams cross vertically, whereas in IP5 and IP8 they cross horizontally.

| Date | Fill | Type | E [TeV] | β^* [m] | Tunes | | | | Xing [μrad] | | | |
|---------------------------|------|----------------|---------|---------------|---------|---------|---------|---------|--------------------------|------------------|-----|------|
| | | | | | Q_x^n | Q_y^n | Q_x^d | Q_y^d | IP1 | IP2 | IP5 | IP8 |
| 26 th Mar. '16 | 4729 | physics | 6.5 | 11.0 | 0.28 | 0.31 | 0.268 | 0.325 | 0 | 0 | 0 | 0 |
| 10 th May '16 | 4908 | VdM | 6.5 | 19.2 | 0.31 | 0.32 | 0.298 | 0.335 | -140 | 200 | 140 | -170 |
| 16 th Jun. '16 | 5023 | high β^* | 6.5 | 2500 | 0.28 | 0.31 | 0.271 | 0.325 | 0 | 200 | 0 | -200 |
| 28 th Jul. '16 | 5124 | ATS | 6.5 | 0.40 | 0.28 | 0.31 | 0.265 | 0.322 | 0 | 0 | 0 | 0 |
| 3 rd Oct. '16 | 5356 | ATS | 6.5 | 0.21 | 0.28 | 0.31 | 0.265 | 0.322 | 0 | 200 | 0 | -250 |
| 20 th Oct. '16 | 5434 | ions | 6.5 | 0.60 | 0.31 | 0.32 | 0.295 | 0.332 | 0 | 138 | 0 | -180 |
| 3 rd Nov. '18 | 7396 | ions | 6.5 | 0.50 | 0.31 | 0.32 | 0.298 | 0.335 | 160 | 137 ^a | 160 | -170 |

^a The measurements of Beam 1 are performed after a crossing angle switch to $-137 \mu\text{rad}$.

reads

$$\sigma_z^2 = \epsilon_z \beta_z + \eta_{z,1}^2 \sigma_p^2 + 3 \eta_{z,2}^2 \sigma_p^4, \quad (7)$$

where ϵ_z and β_z refer to the normalised emittance and the β -function, respectively. To avoid luminosity reduction $\eta_{z,1}$ is generally matched to exact 0 at the IP, neglecting however $\eta_{z,2}$ and possible arising effects. In addition, unexpected σ_z growth must be avoided to guarantee machine protection.

The High Luminosity LHC (HL-LHC) is planned to operate using an Achromatic Telescopic Squeezing (ATS) optics [8]. $\eta_{y,1}$ is corrected using orbit bumps, leading also to a damping of $\eta_{y,2}$, whereas the latter is also damped by the adjacent arcs without applied orbit bumps, as seen in Fig. 2 for ATS optics model calculations of Beam 1 with $\beta^* = 40$ cm and crossing angles in IP1 and IP5. Future measurements with non-zero crossing angles can be performed to validate this behaviour.

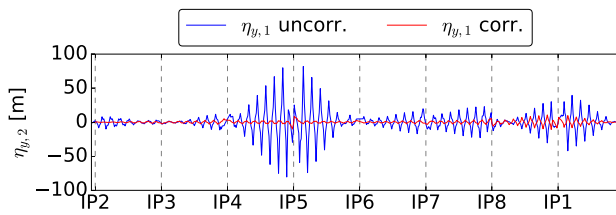


Figure 2: Reduction of $\eta_{y,2}$ in ATS optics with $\beta^* = 40$ cm before (blue) and after (red) correction of $\eta_{y,1}$.

MEASUREMENT AND ANALYSIS

Optics measurements can be performed by exciting the beam with an AC-Dipole [9] and acquiring the Turn-by-Turn (TbT) data at each BPM [10]. Before performing harmonic analysis with methods like SUSSIX [11, 12] or HARPY [13], the data is cleaned using algorithms based on Singular Value Decomposition (SVD). The output includes the measured CO at each BPM. δ_p is computed by $\eta_{x,1}^{mdl}$, obtained by

MAD-X [14], and the measured CO_x through

$$\delta_p = \frac{\langle \eta_{x,1}^{mdl} CO_x \rangle}{\langle (\eta_{x,1}^{mdl})^2 \rangle}, \quad (8)$$

where the denominator is chosen to remain unequal to 0, as $\eta_{x,1}$ is not strictly positive. $\eta_{x,1}^{mdl}$ is chosen over $\eta_{y,1}^{mdl}$, as the latter is expected to be significantly smaller and oscillating around 0. $\eta_{x,2}$ is neglected as tracking studies for the LHC found a discrepancy of about 1% between the expected and the measured δ_p using Eq. (8) and calculating dispersion up to second order. Data with different δ_p can be generated by change of the RF-frequency. $\eta_{z,n}$ is then calculated at every BPM by a polynomial fit of the measured CO_z over various δ_p , where $n+2$ different δ_p are required to fit dispersion and the respective variances up to the order of n . Therefore, at least 4 different δ_p are necessary to compute up to $\eta_{z,2}$, as $n=2$. For the here presented results, data of 7 fills are

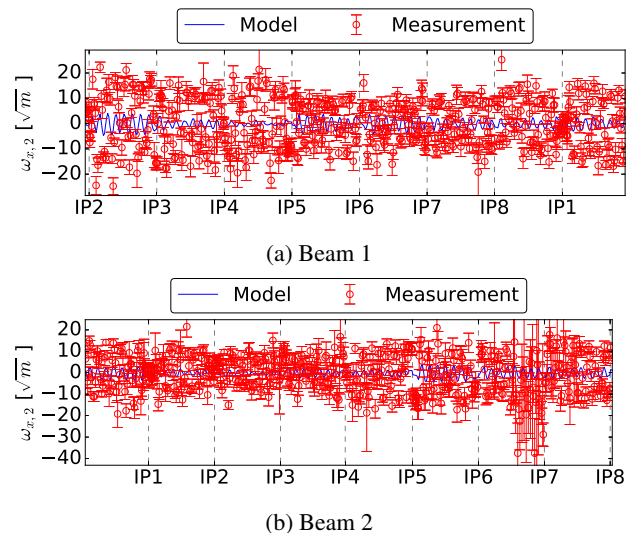


Figure 3: Normalised horizontal second-order dispersion for both beams using ion optics with $\beta^* = 60$ cm.

Content from this work may be used under the terms of the CC BY 3.0 licence (© 2019). Any distribution of this work must maintain attribution to the author(s), title of the work, publisher, and DOI

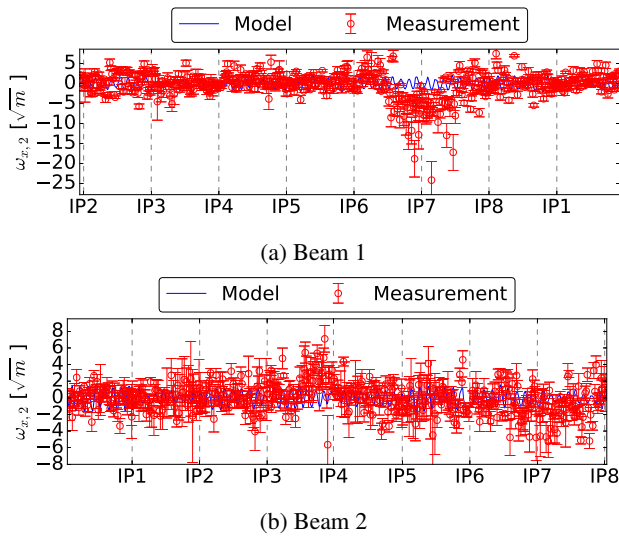


Figure 4: Normalised horizontal second-order dispersion for both beams using proton optics with $\beta^* = 19.2$ m.

analysed, where in total 5 different optics have been used for the measurements. A summary of the analysed measurements can be found in Table 1, where great emphasis is put into choosing the exact crossing scheme in the analytical MAD-X model.

On the one hand, the measured $\omega_{x,2}$ agrees in general well with the model in all fills. Nevertheless, larger $\eta_{z,2}$ than predicted is measured in ion optics with $\beta^* = 60$ cm in 2016, as well as in Van der Meer optics with $\beta^* = 19.2$ m, Beam 1. For ion optics the measured $\omega_{x,2}$, analysed after applying local and global corrections, is about a factor 10 to 20 larger over the whole ring than the MAD-X model, as seen in Fig. 3. Even by enlarging the crossing angles in IP1 and IP5 up to 200 μ rad, $\eta_{x,2}$ increases by only 10 % and can therefore not explain the seen discrepancies. This effect is

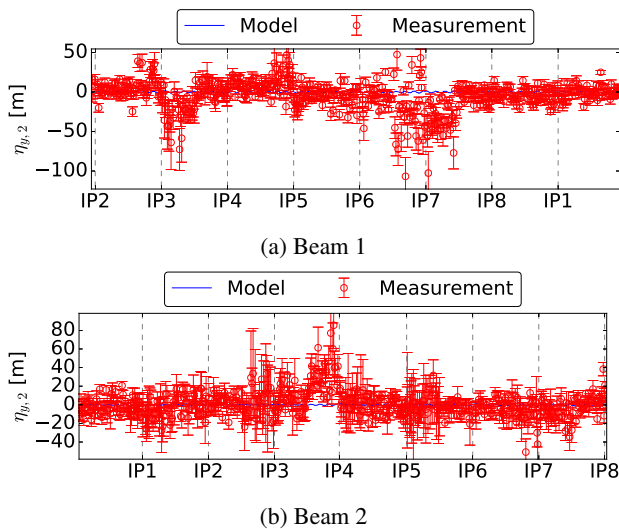


Figure 5: Vertical second-order dispersion for both beams using proton optics with $\beta^* = 19.2$ m.

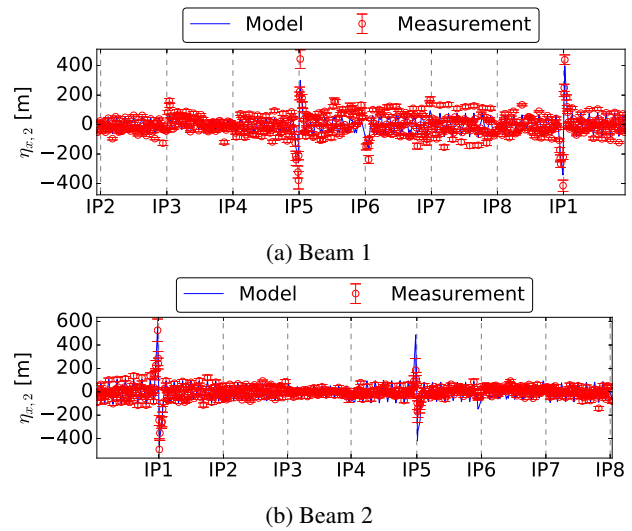


Figure 6: Horizontal second-order dispersion for both beams using ATS optics with $\beta^* = 21$ cm.

not systematic in ion optics as it is not observed in 2018 with $\beta^* = 50$ cm. Unexpected $\omega_{x,2}$ of 20 $\sqrt{\text{m}}$, corresponding in this case to $\eta_{x,2} = 200$ m, leads to an orbit offset of about 150 μm , assuming $\delta_p = 8.6 \times 10^{-4}$ [1]. A $\omega_{x,2}$ peak around Interaction Region (IR) 7 is observed in Van der Meer optics with $\beta^* = 19.2$ m for Beam 1, which is not measured in Beam 2, as seen in Fig. 4. In addition, a vertical second-order dispersion peak is observed for Beam 1 around IR7.

On the other hand, $\eta_{y,2}$ is found to be significantly larger than predicted for the analysed proton optics, as seen in Fig. 5. Moreover, the above mentioned peak around IR7 is observed for Beam 1, where another peak between IR3 and IR4 is located. These peaks exceed the predictions by a maximum factor of about 80. In case of Beam 2 a larger $\eta_{y,2}$ is observed left of IR4.

The largest $\eta_{x,2}$ is found using ATS optics with $\beta^* = 21$ cm, where the maxima of about 500 m are located close to IP1 and IP5, as seen in Fig. 6. At the IPs however, $\eta_{x,2}$ is about 5 m, which results in an additional orbit offset of 4 μm , with $\delta_p = 8.6 \times 10^{-4}$, whereas the beam size growth can be neglected. In addition, $\eta_{y,2}$ exceeds the model predictions by about 150 m close to the main experiments.

CONCLUSION

For the first time in the LHC, second-order dispersion has been measured. Data of seven fills with different optics have been analysed and compared with the respective models, and in general, a good agreement between the measurements and the model is found. In case of arising discrepancies, second-order dispersion peaks are found close to the main experiments, where possible error sources could be uncorrected non-linear errors, strong non-linear elements or uncorrected coupling. Investigations to identify global and local second-order dispersion knobs and correction techniques are ongoing to avoid unexpected orbit offsets and beam size growth in future operations.

REFERENCES

- [1] O. Brüning *et al.*, "LHC Design Report", CERN, Geneva, CERN Yellow Reports, Monographs, 2004.
- [2] H. Wiedemann, "Particle Accelerator Physics", 4th Edition, Springer International Publishing Switzerland, 2015.
- [3] J. P. Delahaye and J. Jäger, "Variation of the Dispersion Function, Momentum Compaction Factor, and Damping Partition Numbers with Particle Energy Deviation", *Part. Accel.* **18**, pp. 183-201, 1985.
- [4] A. Franchi, S. M. Liuzzo and Z. Martí, "Analytic Formulas for the Rapid Evaluation of the Orbit Response Matrix and Chromatic Functions from Lattice Parameters in Circular Accelerators", arXiv:1711.06589v2, 2018.
- [5] A. Wolski, "Beam Dynamics in High Energy Particle Accelerators", Imperial College Press, 2014.
- [6] R. Calaga, R. Tomás, and F. Zimmermann, "BPM Calibration Independent LHC Optics Correction", in *Proc. 22nd Particle Accelerator Conf. (PAC'07)*, Albuquerque, NM, USA, Jun. 2007, paper THPAS091, pp. 3693-3695.
- [7] A. Garcia-Tabares *et al.*, "MD Test of a Ballistic Optics", CERN-ACC-NOTE-2016-0008, 2016.
- [8] S. Fartoukh, "Achromatic Telescopic Squeezing Scheme and Application to the LHC and its Luminosity Upgrade", *Phys. Rev. Accel. Beams* **16**, p. 111002, 2013. doi:10.1103/PhysRevSTAB.16.111002
- [9] M. Bai *et al.*, "Overcoming Intrinsic Spin Resonances with an RF Dipole", *Phys. Rev. Lett.* **80**, p. 4673, 1998.
- [10] R. Tomás, M. Aiba, A. Franchi and U. Iriso, "Review of Linear Optics Measurement and Correction for Charged Particle Accelerators", *Phys. Rev. Accel. Beams* **20**, p. 054801, 2017. doi:10.1103/PhysRevAccelBeams.20.054801
- [11] R. Bartolini and F. Schmidt, "A Computer Code for Frequency Analysis of Non-Linear Betatron Motion", CERN, Geneva, Switzerland, Report CERN-SL-NOTE-98-017-AP, 1998.
- [12] T. Bach and R. Tomás, "Improvements for Optics Measurements and Corrections Software", CERN, Geneva, Switzerland, Report CERN-ACC-NOTE-2013-0010, 2013.
- [13] L. Malina, J. M. Coello de Portugal, J. Dilly, P. K. Skowroński, R. Tomás, and M. S. Toplis, "Performance Optimisation of Turn-by-Turn Beam Position Monitor Data Harmonic Analysis", in *Proc. 9th Int. Particle Accelerator Conf. (IPAC'18)*, Vancouver, Canada, Apr.-May 2018, pp. 3064-3067. doi:10.18429/JACoW-IPAC2018-THPAF045
- [14] MAD-X, <http://mad.web.cern.ch/mad/>.